A sub-millimeter spatial resolution achieved by a large sized glass RPC *

LI Qi-Te(李奇特) YE Yan-Lin(叶沿林)[1)] JI Wei(纪玮) WEN Chao(文超)
LIU Hong-Tao(刘洪涛) GE Yu-Cheng(葛愉成)
School of Physics and State Key Laboratory of Nuclear Physics and Technology, Peking University, Beijing 100871, China

Abstract: Three large sized glass resistive plate chambers (RPCs) are built and applied to measure the spatial resolution of the detector. The readout strips are collected to a LC delay-line and the time difference is used to determine the position. Cosmic rays are triggered by a set of two scintillation counters and the coincidently measured positions from the three RPCs are used to deduce the position uncertainty. In average a spatial resolution of 0.90 mm (FWHM) is obtained for a single RPC, with a good uniformity across the detection area. This result suggests that large sized glass RPC operating in the avalanche mode is a promising candidate for the muon tomography detection system.

Key words: RPC, spatial resolution, cosmic ray, delay-line

PACS: 29.40.Cs, 29.40.Gx, 29.40.Mc **DOI:** 10.1088/1674-1137/37/1/016002

1 Introduction

In the 1980s, a new type of large sized gas detector, the resistive plate chamber(RPC), was developed [1], allowing us to obtain good time resolution as an alternative to the "localized discharge spark counter" [2]. Over the years it has been proved that large sized RPCs have many advantages such as a simple and robust structure, long time stability, good time resolution, easy-maintenance and low cost [3–5]. Based on intensive studies large sized RPCs have been widely used in high energy physics experiments such as CMS at LHC [6, 7], cosmic-ray experiments such as ARGO-YBJ [8] and neutrino experiments such as OPERA [9]. In recent years small sized timing RPCs have also been developed [10, 11] and applied to experiments such as ALICE [9], HADES [12] and FOPI [13]. These applications require very high counting rates or excellent timing resolutions, but only moderate spatial resolutions (a few centimeters). As a result, spatial resolution has not been well studied so far for large sized RPCs [5, 14].

Since the last ten years muon tomography (MT) has attracted much attention due to its possible application in detecting high Z materials, which is closely related to national security programs [13, 14]. Precise measurements of the incident and outgoing angles of the cosmic muons are mandatory in this application, which normally requires a sub-millimeter spatial resolution for the applied tracking detectors. There are several testing facilities of MT using drift tubes [15], drift chambers [16] and gas electron multiplier detectors [17]. These detectors are relatively complex and expensive, and often require a very large number of electronic channels for a realistic application system. Very recently we began to investigate the possibility of using large sized RPC for the MT purpose, due to its simplicity, robustness and low cost. Despite its advantages, the most important question to be solved is of course its achievable spatial resolution. At first we have studied the properties of signal profile generated by the cosmic muon in the gas volume of a large sized glass RPC [18]. The size of the profile should in principle put an intrinsic limit to the spatial resolution of the detector. Both streamer mode signals and avalanche mode signals were tested. As expected the latter ones give a much smaller profile size than the former ones. A FWHM of about 4 mm was obtained for the avalanche signal profile, indicating a possibility of determining the signal peak position with a precision of less than 1 millimeter [18]. But this was just an estimation based on the measurements of the signal properties of one RPC. The real spatial resolution must come from measurements with several layers of detectors which record the real tracks.

In this rapid communication we report the observation of the sub-millimeter spatial resolution for the large sized glass RPC, based on the measurements with a stack

Received 2 March 2012
∗ Supported by National Natural Science Foundation of China (11035001, 10827505, 10775003)
1) E-mail: yeyl@pku.edu.cn

of three RPCs. We give descriptions of the detector setup and their performance in Section 2, and the measurements and results in Section 3.

2 Description of the detector setup

The detailed design and assembly of the prototype glass RPC were described in Ref. [18], which were repeated for all three RPCs used here. As shown in Fig. 1, the gas chamber of the RPC is formed by two float glass plates, each with a thickness of 2.6 mm. The gas gap between the plates is 2 mm thick, fixed by spacers. The high voltage (HV) electrode is made by a thin layer of graphite coated on each of the glass plates with a surface resistivity of about $10^7\Omega$/sq. Each of the graphite layers is covered by a 100 μm PET film for insulation. The effective area of the plate is 200 mm×200 mm. The read-out strips are integrated on a printed-circuit board which is placed beneath the gas gap. For this test measurement the strip layer spans only half of the active chamber area, covering 200 mm×100 mm, due to the application of another half of the chamber area for other studies.

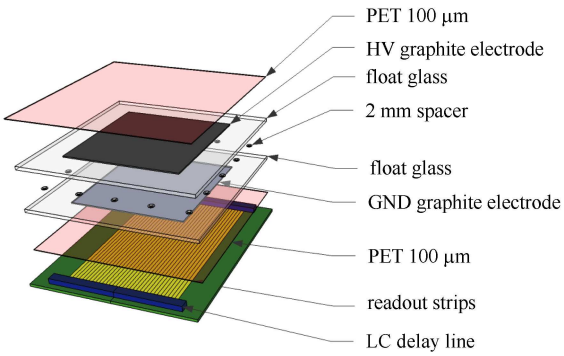

Fig. 1. Layout of the prototype glass RPC.

As the counting rate is relatively low for cosmic ray detection, we may apply the delay-line or charge-division method which allows us to largely reduce the number of readout channels and related electronics. In the meantime these methods may lead to an extraordinarily good spatial resolution through the determination of the centroid of the signal charge profile, meaning much better than the strip width or wire spacing [14, 19, 20]. The design of the readout strip width depends on the size of the signal profile [21]. We have experimentally measured this profile through the centroid matching method and the results were reported in Ref. [18]. To obtain the induced charge profile, we fed signals of 10 strips with 2 mm spacing to QDC. For each event, we determine the center of the distribution (X_c) by using the charge weighted average method. For each fired read-out strip the X position is determined according to its distance to the center ($X-X_c$), while the vertical coordinate is the ratio of the readout charge taken from that strip relative to the total charge of the signal. Fig. 2 shows the profile for avalanche signals, which has a width (FWHM) of about 4 mm. According to this measurement we arranged a readout strip pitch of 2.54 mm, so the induced charge profile can be sampled by several readout strips, allowing us to determine the centroid with a high accuracy.

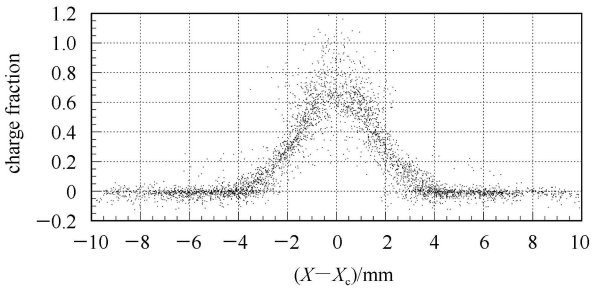

Fig. 2. The induced charge profiles for avalanche signals. The FWHM of the profile is about 4 mm.

In this work we adopt the delay-line method. Between every two adjacent strips a delay of 4 ns is realized by connecting the strips to a commercial LC delay-line (type 1507-40A). Each delay-line unit has 10 taps, with each having a fixed delay of 4.0 ns. Signals from both ends of a delay-line are fed into the 300 MHz fast preamplifiers, and then sent to the timing electronics circuit [18]. The position of a crossing particle is then obtained by the time difference between the two signals taken from both ends of the delay-line. The delay-line is calibrated by sending pulser signals into various connection points of the delay-line and measuring the time differences at the both ends. It is found that the non-linearity of the time difference versus position is less then 1%. It must be noted here that we put read-out strips only in one direction and therefore only the one-dimensional position can be measured with the current setup. For two-dimensional measurement, more layers of RPCs with crossing strips should be used.

All three RPCs are stacked inside an aluminum box (Fig. 3) with the same distance between any two neighboring RPCs. The readout strips are in the same direction for all three layers. The box is equipped with HV, signal and gas in-out connectors. The applied gas mixture was studied previously and the adopted best composition is 90% F_{134a}+9% iso-C_4H_{10}+1% SF_6, with a flow rate of about 50 cm^3/min. The HV supplied to each RPC was 9700 V which assures an avalanche mode operation of the chamber as tested in the previous work [18].

3 Measurement and result

Each of the RPCs were tested against the dark current and efficiency performance. Also, the previously

tested signal profile and delay-line uniformity provide a good base for determining the position resolution [18].

For a real position resolution measurement, normally a small collimated radiation source is required. However, this method is not practical for a cosmic ray experiment due to the very low counting rate for a small collimation hole (or slit). Here we adopt a more effective approach relying on the measurement of all cosmic-ray tracks passing through the whole system with at least three layers of similar detectors [22, 23]. As shown in Fig. 3 two scintillation counters were placed on the top of the RPC system, in a direction parallel to the strips. Cosmic rays triggered by these scintillators can irradiate over the whole size of the RPC with little different incident angles. Here we show a position spectrum measured by one of the RPCs (Fig. 4) for coincidently detected cosmic rays. The spectrum has a shape as expected from the triggered cosmic ray distribution.

For each good event, three positions X_1, X_2 and X_3 are obtained from the three RPCs, respectively. The residual can be defined as:

$$\Delta X = X_2 - \frac{X_1+X_3}{2}, \tag{1}$$

which is the difference between the directly measured position X_2 and that projected from X_1 and X_3. A spectrum on ΔX was accumulated for all coincidently measured events, as shown in Fig. 5(e). Offsets of the

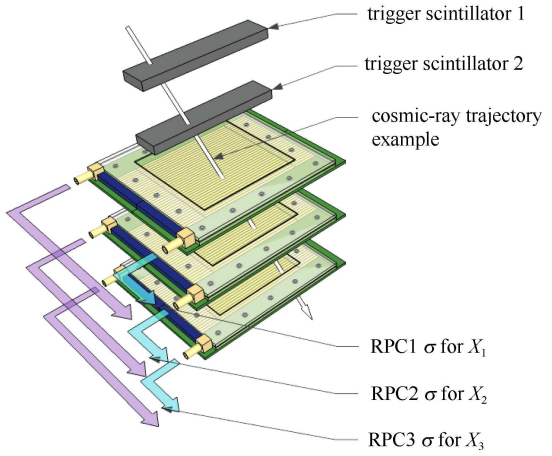

Fig. 3. Schematic view of the detection system with three RPCs.

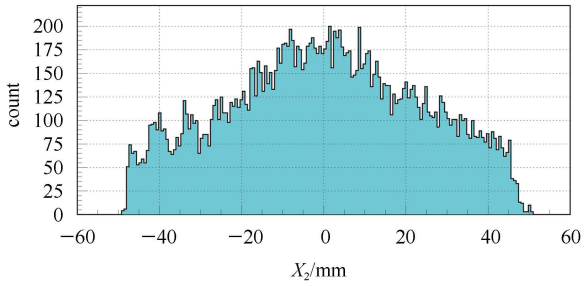

Fig. 4. Position spectrum taken from one RPC.

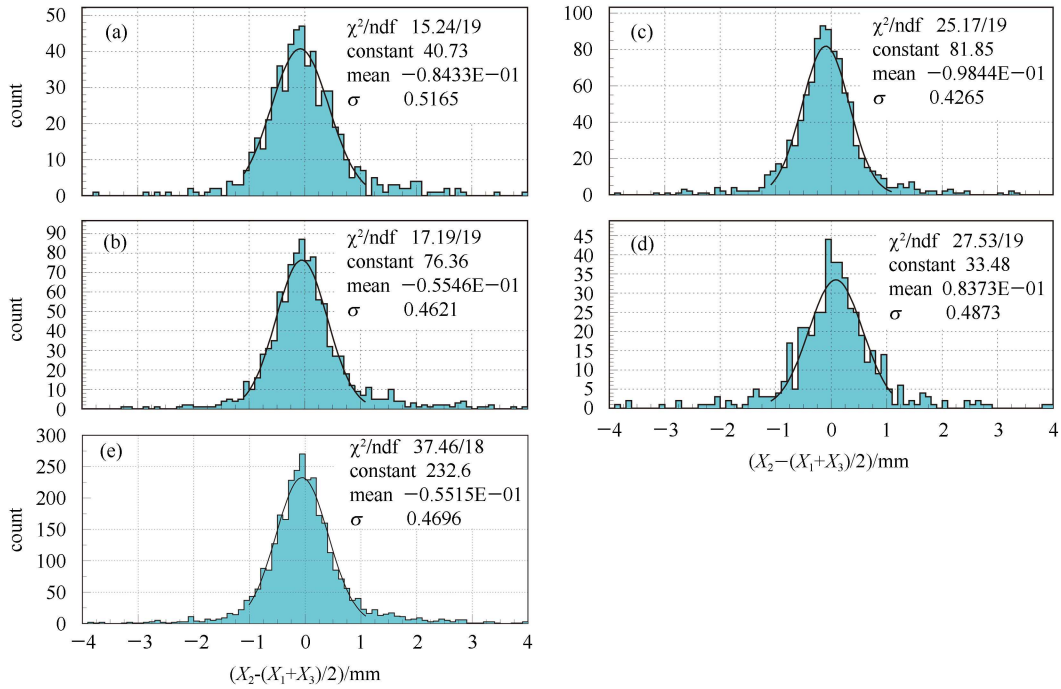

Fig. 5. Spectra for position residuals deduced from positions measured by three RPCs (see Eq. (1)), with Gaussian function fits. The readout strip area along the X position is divided into four sections: −50 to −25 mm region (plot (a)); −25 to 0 mm region (plot (b)); 0 to 25 mm region (plot (c)) and 25 to 50 mm region (plot (d)). The overall distribution is given in plot (e), with the Gaussian function parameter σ=0.470 mm (FWHM=1.10 mm).

positions can be fixed by adjusting the center of the spectrum peak at zero, whereas the average uncertainty of the position determination is naturally given by the width of the peak. According to a Gaussian function fit as shown in Fig. 5(e), the actual FWHM of the peak is 1.10 mm, which is contributed from all three RPCs. Treating the three RPCs equally, each should then have a spatial resolution (FWHM) of $\sqrt{\frac{2}{3}}*1.10$=0.90 mm. This result is very close to the previously estimated intrinsic position resolution [18]. A very small tail at the right side of the peak might be attributed to the small nonlinearity of the delay-line, which could further be improved by using better delay-line units.

In order to demonstrate the uniformity of position resolution along the LC delay-line, we divided the X position of the middle RPC (Fig. 4 as an example) into four sections: -50 to -25 mm, -25 to 0 mm, 0 to 25 mm and 25 to 50 mm, respectively. We built a residual spectrum for each of the four sections. The results are shown in Fig. 5(a), 5(b), 5(c) and 5(d), respectively. The Gaussian fits give σ=0.517 mm, 0.462 mm, 0.427 mm, and 0.487 mm, corresponding to FWHM=1.212 mm, 1.086 mm, 1.001 mm and 1.144 mm. Again from the residual distribution we can get the chamber spatial resolutions of 0.99 mm, 0.89 mm, 0.82 mm and 0.93 mm for the four sections, respectively. These results show quite good uniformity of the RPCs, with a little larger spatial resolution at both sides of the chamber in comparison with the middle sections. This is normal since the delay units can appreciably attenuate and distort signals.

4 Summary

Three large sized glass RPCs were built and applied to measure the spatial resolution of the detector. The readout strips are collected to a LC delay-line and the time difference method was used to determine the position. Cosmic rays were triggered by a set of two scintillation counters and the coincident positions recorded by three RPCs were used to deduce the position uncertainty. An average spatial resolution of 0.90 mm (FWHM) can be obtained for one RPC. The uniformity of the spatial resolution is also checked for different areas of the RPC chamber , and a little larger , but all below 1 mm (FWHM) spatial resolutions at both sides of the chamber are identified in comparison to the middle sections. This result suggests that the large sized glass RPC operating in avalanche mode is a promising candidate for a muon tomography detection system. It is highly encouraged to further extend the actual test setup to a complete tracking system to show its imaging capability.

References

1 Santonico R, Cardarelli R. Nucl. Instrum. Methods A, 1981, **187**: 377
2 Parkhomchuck V V, Pestov Yu N, Petrovykh N V. Nucl. Instrum. Methods, 1971, **93**: 269–276
3 Fonte P. IEEE Trans. Nucl. Sci., 2002, **49**: 881
4 Santonico R. Nucl. Phys. B, 2006, **158**: 5
5 Santonico R. Nucl. Instrum. Methods A, 2012, **661**: S2–S5
6 YING J, YE Y L, BAN Y et al. Nucl. Instrum. Methods A, 2001, **459**: 513–522
7 Aftab Z et al. Nucl. Phys. B, 2006, **158**: 103–107
8 Aielli G et al. Nucl. Instrum. Methods A, 2012, **661**(Suppl. 1): S56–S59
9 Bertotin A et al. Nucl. Instrum. Methods A, 2009, **602**: 631
10 Finck C et al. Nucl. Instrum. Methods A, 2003, **508**: 63–69
11 Blanco A et al. Nucl. Instrum. Methods A, 2003, **508**: 70–74
12 Aamodt K et al. J. Instr., 2008, S08005
13 Schuttaut A et al. Nucl. Instrum. Methods A, 2009, **602**: 679
14 Santonico R. Nucl. Instrum. Methods A, 2004, **533**: 1–6
15 Morris C L, Alexander C C, Bacon J D et al. Science and Global Security, 2008, **16**: 37
16 Anghel V et al. Nuclear Science Symposium Conference Record (NSS/MIC), 2010, IEEE Issue Date: Oct. 30 2010-Nov. 6 2010, On page(s): 547–551
17 Gnanvo K et al. Nucl. Instrumu. Methods A, 2011, **652**: 16–20
18 LI Q T, YE Y L, WEN C et al. Nucl. Instrum. Methods A, 2012, **663**: 22–25
19 Assamagan K et al. Nucl. Instrum. Methods A, 1999, **426**: 405–419
20 YE Y L, DI Z Y, LI Z H et al. Nucl. Instrum. Methods A, 2003, **515**: 718–724
21 Smith G C et al. IEEE Trans. Nucl. Sci., 1988, **35**: 409–413
22 Blaich Th, Elze Th W, Embling H et al. Nucl. Instrum. Methods A, 1992, **314**: 136–154
23 YANG Z H, YE Y L, XIAO J et al. Chin. Phys. C (HEP & NP), 2012, **36**: 1–6